

A facile strategy for obtaining fresh Ag as SERS active substrates

Zibao Gan^{a,b,c}, Aiwu Zhao^{a,b,c,*}, Maofeng Zhang^{b,c}, Dapeng Wang^{b,c}, Wenyu Tao^{a,b,c}, Hongyan Guo^{b,c}, Da Li^{b,c}, Ming Li^{a,b,c}, Qian Gao^{b,c}

^a Department of Chemistry, University of Science and Technology of China, Hefei 230026, Anhui, PR China

^b Institute of Intelligent Machines, Chinese Academy of Sciences, Hefei 230031, PR China

^c State Key Laboratory of Transducer Technology, Chinese Academy of Sciences, Hefei 230031, PR China

ARTICLE INFO

Article history:

Received 7 July 2011

Accepted 21 September 2011

Available online 29 September 2011

Keywords:

SERS

Fresh Ag

Irradiation time

4-Mercaptopyridine

ABSTRACT

A facile strategy has been reported to obtain on-line fresh Ag as surface-enhanced Raman scattering (SERS) active substrates by making AgCl nanoparticles exposed to the laser beam of Raman spectrometer. The composition and morphology of AgCl nanoparticles were characterized by X-ray diffraction (XRD), UV–visible (UV–vis) spectroscopy and scanning electron microscopy (SEM). The laser-driven evolution and possible formation mechanism of cubic AgCl nanoparticles to Ag/AgCl composites were also investigated by transmission electron microscopy (TEM), energy dispersive X-ray spectroscopy (EDS) and high-resolution transmission electron microscopy (HRTEM). Raman measurements demonstrate that the fresh Ag nanoparticles with a few defects have a prominent SERS sensitivity to probe molecules, such as the 4-mercaptopyridine (4-Mpy) and 4-aminothiophenol (PATP) molecules. The SERS intensity of 4-Mpy and PATP increases up to the maximum when the laser irradiation time is prolonged to 50 s, which corresponds to the defect extent and the proportion of fresh Ag in the Ag/AgCl composites. This work provides a simple, efficient and feasible approach for obtaining on-line fresh Ag as SERS substrates.

© 2011 Elsevier Inc. All rights reserved.

1. Introduction

Since its initial discovery, surface-enhanced Raman spectroscopy (SERS) has displayed tremendous potential in structural analysis, nanotechnology and biological sensing [1–5]. For its prominent exhibition, the study on SERS-based substrates has been extensively investigated in the past decades [6,7]. Among the various substrates, Ag is a superior candidate as SERS substrate due to its advantage of high Raman enhancement factor. It is known that the origin of enhancement effect is attributed to two mechanisms: the local electromagnetic field enhancement as a result of excitation of the surface plasmon and the chemical adsorption of probe molecules on the surface of the substrates [8,9]. According to the electromagnetic mechanism, the SERS performances are strongly dependent on their shape, size and surface morphology. As a result, many efforts have been made to synthesize Ag nanostructures with tunable size and morphology. For example, Xia and co-authors synthesized 30–200 nm Ag nanocubes with better SERS properties [10]. Driskell et al. fabricated aligned Ag nanorod arrays as SERS substrates [11]. Liu and co-workers reported an active, stable and biocompatible Ag nanofilm SERS substrates [12]. Recently, our group also reported a few simple methods to synthesize

three-dimensional (3D) flower-like and rosette-like silver nanocrystals with textured surface topography as sensitive SERS substrates [13,14]. It is reported that the Ag substrates with better SERS properties are easy to suffer oxidation and be spotted under the normal circumstances, which can tremendously decrease their SERS performances [15]. Thus, it is a challenge to seek alternative methods to obtain fresh Ag as efficient SERS substrates.

New findings show that fresh Ag nanoparticles obtained by decomposition of silver halide can serve as sensitive SERS substrates [16]. Researches have pointed out that the SERS activity is essentially contributed by the silver clusters generated from the photochemical decomposition of silver halide colloids, which has been accepted by most groups [16,17]. Recently, Yang et al. also reported a new SERS active silver substrate with great defects prepared by iodination of the evaporated silver foil [18]. Nevertheless, the study on obtaining fresh Ag nanoparticles as SERS substrates has received little attention.

Inspired by the above strategies, a newly modified laser-driven decomposition strategy was developed to obtain on-line fresh Ag as SERS active substrates. In this paper, cubic AgCl nanostructures were firstly prepared by a simple aqueous solution method. Then, the fresh Ag nanoparticles were obtained on-line by making AgCl nanoparticles exposed to the laser beam of Raman spectrometer. The laser-driven evolution and possible formation mechanism of cubic AgCl precursors to Ag/AgCl composites were amply investigated by TEM, EDS and HRTEM. The fresh Ag nanoparticles with a

* Corresponding author at: Institute of Intelligent Machines, Chinese Academy of Sciences, Hefei 230031, PR China. Fax: +86 551 5592420.

E-mail address: awzhao@iim.ac.cn (A. Zhao).

few defects make a significant contribution to the sensitivity of SERS to probe molecules, such as 4-mercaptopyridine (4-Mpy) and 4-aminothiophenol (PATP) molecules. Raman results show that Raman intensity is dependent on the defect extent and the proportion of fresh Ag in the Ag/AgCl composites. When the laser irradiation time is prolonged to 50 s, the SERS intensity of 4-Mpy and PATP increases up to the maximum. Moreover, the cubic AgCl nanoparticles stored for 100 days in dark room can still serve as an efficiency detection platform under the drive of laser.

2. Materials and methods

2.1. Materials and chemicals

Silver nitrate (AgNO_3), sodium chloride (NaCl) and polyvinylpyrrolidone (PVP, Mw = 58,000) were purchased from Sinopharm Chemical Reagent Co., Ltd., China. 4-Mpy and PATP were supplied by Aladdin Reagent Co. All the chemicals were analytic grade and used as-received without further purification. The ultrapure water used in the experiments has a resistivity of 18.2 M Ω cm and was produced from a Millipore Milli-Q system.

2.2. Synthesis of cubic AgCl nanoparticles

Cubic AgCl nanoparticles were synthesized by a simple aqueous solution method. In a typical synthesis, 0.0333 g PVP was added into 20 mL of AgNO_3 (5 mM). After stirring for 15 min, 0.0058 g NaCl was rapidly added into the above solution. Immediately, it turned white. After reacting for 30 min, the white sediments were collected by centrifuging and washing with water and ethanol. Finally, the products were dispersed into ethanol and conserved in dark room for further characterization.

2.3. Adsorption of probe molecules

The as-received sample solutions were carefully dropped on the specially cleaned glass slides. After the above solutions were completely dried in dark room, 45 μL of 4-Mpy solutions (1.0×10^{-5} M) and 45 μL of PATP solutions (5.0×10^{-5} M) were dropped onto the above substrates, respectively. The 4-Mpy and PATP molecules were naturally adsorbed and dried in dark room for further Raman studies.

2.4. Characterization

X-ray diffraction (XRD) patterns of the as-received samples were recorded on a Bruker D8 Focus diffractometer with Cu K α radiation operated at 40 kV and 40 mA. UV-Visible (UV-vis) absorption spectrum of the products was obtained with a UV-4802 spectrophotometer. Scanning electron microscopy (SEM) was conducted on an FEI Sirion-200 field emission scanning electron microscope. Energy dispersive X-ray spectroscopy (EDS) was conducted on an H-7650 transmission electron microscope (TEM) with an energy dispersive X-ray detector. High-resolution transmission electron microscopy (HRTEM) was realized on a JEL-2100 transmission electron microscope at an acceleration voltage of 200 kV. Raman spectra were recorded by a Renishaw 1000 confocal Raman spectrometer with a 532 nm laser beam. The laser beam is focused on a radius of about 1 μm samples. The laser power is 2 mW, and the recording time is 10 s for each spectrum.

3. Results and discussion

3.1. Characterization of AgCl nanoparticles

The XRD patterns of samples were displayed in Fig. 1a. The diffraction peaks are assigned to the (111), (200), (220), (311), (222), (400) and (420) planes of face center cubic (fcc) AgCl, respectively. All the diffraction peaks can be easily indexed to a pure cubic phase [space group Fm-3 m] of AgCl (JCPDS Card No. 31-1238). These planes with sharp peaks demonstrate that the obtained samples are well crystallized. No other impure peaks were detected, indicating the high purity of as-received products. The UV-vis absorption spectrum (inset in Fig. 1a) of products is in good agreement with the reported, which further affirmed that the as-received products are AgCl [19]. Fig. 1b presents a typical SEM image of the AgCl nanoparticles, clearly revealing that most nanoparticles exhibit cubic morphologies and uniform size with average edge length of 300 nm.

3.2. Laser-driven evolvement and possible mechanism illustration

TEM and EDS techniques have been employed to investigate the laser-driven evolvement of cubic AgCl nanoparticles to Ag/AgCl composites. The spots on cubic AgCl nanoparticles continuously irradiated by laser for 10, 30 and 50 s were chosen to actualize

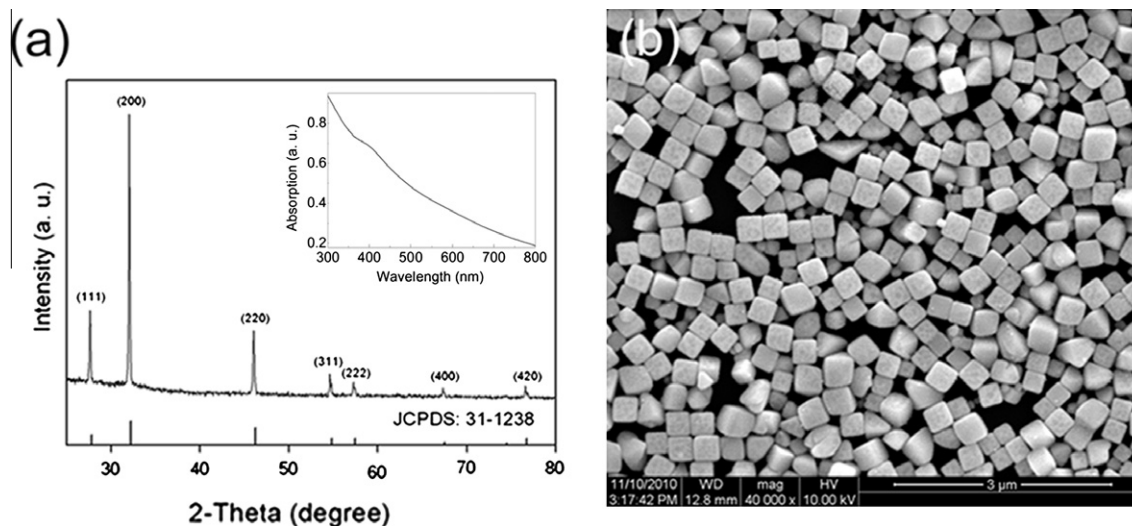


Fig. 1. (a) XRD patterns of samples (the inset shows the UV-vis absorption spectrum); and (b) SEM image of AgCl nanoparticles.

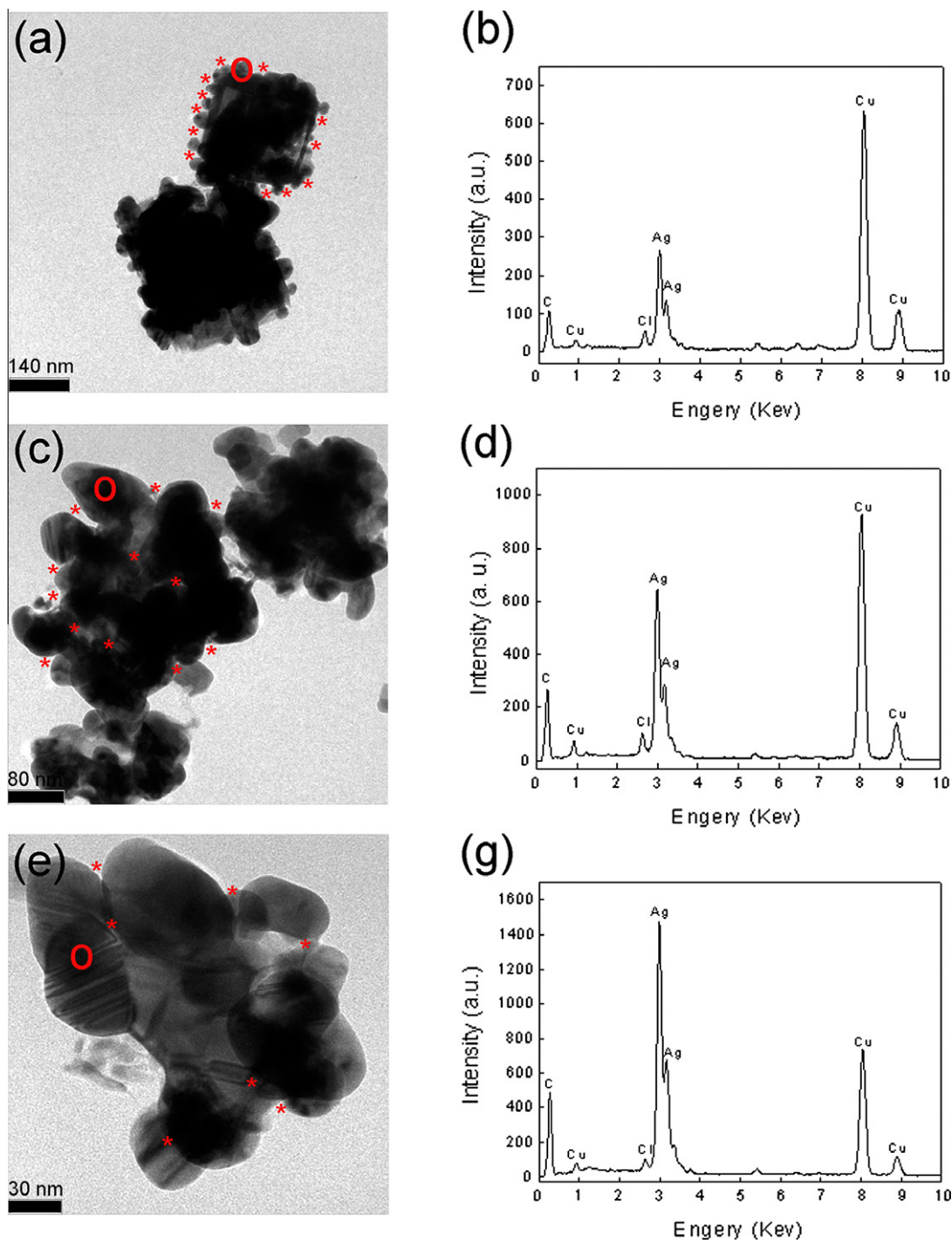


Fig. 2. TEM images and EDS data of AgCl irradiated by laser for different time (a and b) 10 s, (c and d) 30 s, (e and f) 50 s (Each EDS data was collected from the red circle embedded in corresponding TEM image). (For interpretation of the references to color in this figure legend, the reader is referred to the web version of this article.)

TEM and EDS analysis. As shown in Fig. 2a, a large number of irregular particles were produced on the surface of cubic AgCl nanoparticles irradiated by laser for 10 s. Corresponding EDS data demonstrate that the relative atom percentages of Ag and Cl are 89.83% and 10.17%, respectively (Fig. 2b). According to the chemical rule that the amount of all the detectable Cl^{-1} is always equal to Ag^{+1} , we could conclude the molar ratio of Ag/AgCl is 79.66/10.17. Thus, it can be seen that the irregular particles on AgCl surface mainly consist of fresh Ag particles. Besides, HRTEM image shows that these fresh Ag nanoparticles are provided with more defects and no clear lattice stripes has been formed (see Supporting

Fig. S1). It is easy to find that there are a few nanoscale gaps between the neighboring fresh Ag particles with defects (labeled with * in Fig. 2a, c and e), which are usually called “hot spots” for SERS [20]. As the laser irradiation time increases to 30 s, the cubic AgCl nanoparticles begin to disappear along with the appearing of more Ag particles (Fig. 2c). EDS analysis testifies that the molar ratio of Ag/AgCl is increased to 84.6/7.7 (Fig. 2d). After irradiated by laser for 50 s, the surface of cubic AgCl nanoparticles was absolutely peeled off (Fig. 2e) and some small Ag particles evolved into a few big Ag particles. Nevertheless, the molar ratio of Ag/AgCl is up to a maximum for 98.3/0.852 (Fig. 2f). HRTEM image also

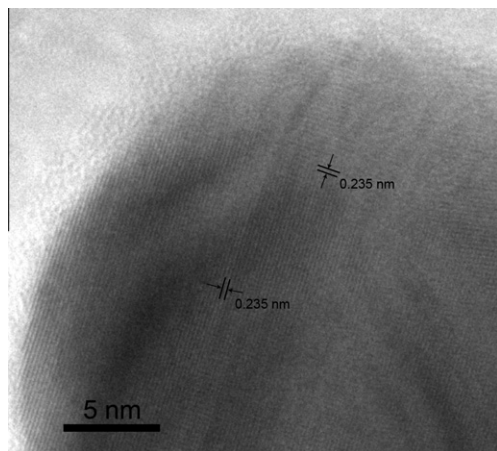


Fig. 3. HRTEM image of AgCl irradiated by laser for 50 s (The data were collected from the red circle embedded in Fig. 2e).

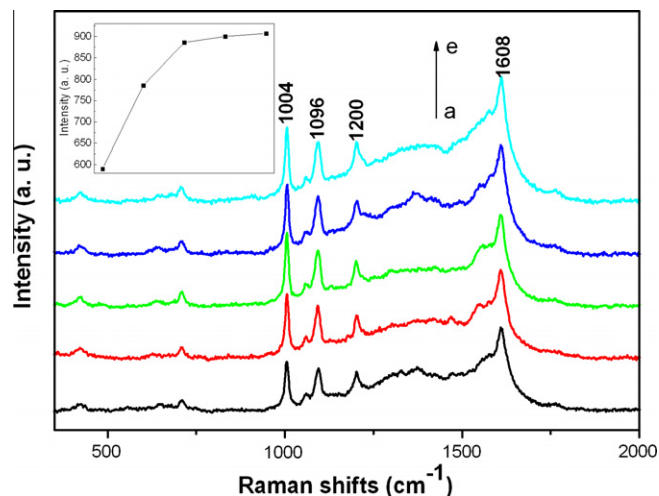


Fig. 6. Raman spectra of 4-Mpy (1.0×10^{-5} M) obtained by continuous irradiation for different time (a) 10 s, (b) 20 s, (c) 30 s, (d) 40 s, and (e) 50 s (The inset shows the intensity of band at 1004 cm^{-1} as a function of irradiation time).

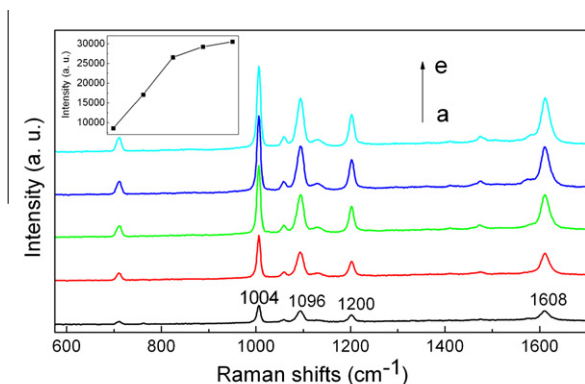


Fig. 4. Raman spectra of 4-Mpy (1.0×10^{-5} M) obtained by continuous irradiation for different time (a) 10 s, (b) 20 s, (c) 30 s, (d) 40 s, and (e) 50 s (The inset shows the intensity of band at 1004 cm^{-1} as a function of irradiation time).

displays that the clear lattice stripes with interplanar spacing of about 0.235 nm have come into being on that big Ag particles, revealing that the growth of the obtained Ag occurs preferentially on (111) plane (Fig. 3) and the cubic AgCl nanoparticles have evolved into stable Ag/AgCl composites with few defects after irradiated by laser for 50 s.

Based on the above discussion, a possible evolution mechanism can be concluded. First, the confocal laser has higher energy intensity rather than other lights. When it was focused on a radius of about $1 \mu\text{m}$ samples, the single cubic AgCl nanoparticle with average edge length of 300 nm was absolutely irradiated so that the fresh Ag particles with defects were produced on AgCl surface in a short time. Second, as the irradiation time increases, the fresh Ag proportion in the Ag/AgCl composites also undergo an increased process. Finally, the Ag proportion is up to a maximum and a coating consisting of the grown Ag particles with few defects came into being, which effectively protects the residual AgCl from decomposition.

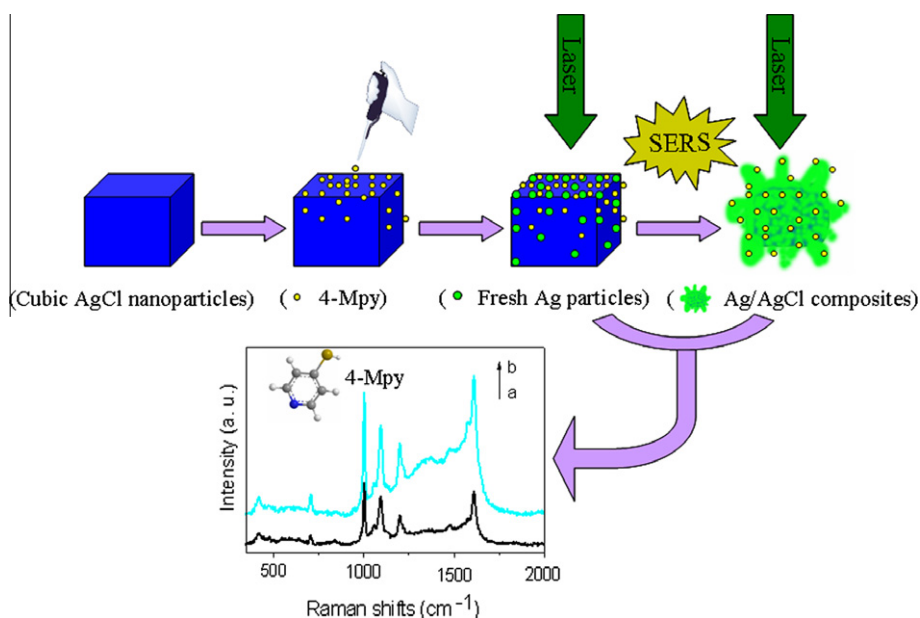


Fig. 5. Schematic illustration of obtaining on-line SERS signals.

Thus, it can be seen that the confocal laser plays a key role in the fast obtaining fresh Ag.

3.3. Raman measurements

The applications of cubic AgCl nanoparticles in SERS were investigated on-line in the same position by using 4-Mpy as probe molecules. Because the UV–vis absorption band of 4-Mpy molecules is situated in 342 nm (see Supporting Fig. S2), while the laser wavelength used in SERS measurements is 532 nm, it avoids the enhancement of 4-Mpy signals caused by the self-resonance of molecule. Fig. 4 shows the Raman spectra of 4-Mpy adsorbed on cubic AgCl nanoparticles. These bands from 500 to 1800 cm^{-1} are attributed to 4-Mpy signals. The bands at 1004, 1200 and 1608 cm^{-1} are assigned to the ring breathing modes, CH/NH deformation modes and pyridine ring C=C stretch modes, respectively [21]. That at 1096 cm^{-1} belongs to so-called X-sensitive modes that are described as modes strongly coupled between substitute and aromatic ring modes [22]. From Fig. 4a–e, it can be seen that the Raman signals of 4-Mpy are enhanced till a maximum as the laser irradiation time is prolonged to 50 s. In order to definitely illustrate the enhancement phenomenon, the intensity of band at 1004 cm^{-1} as a function of irradiation time is exhibited in the inset of Fig. 4. Obviously, the intensity of band at 1004 cm^{-1} is increasingly added to a peak value, but enhancement extent for each time is non-uniform. On the basis of previous reports, the enhancement may ascribe to the EM enhancement caused by the surface plasmon resonance of as-received fresh Ag with defects on cubic AgCl surface [16,17]. When the laser irradiation time is short, fresh Ag nanoparticles with more defects create more “hot spots” so that the enhancement extent is strong. The proportion of fresh Ag nanoparticles is increased as the laser irradiation time is prolonged, but the defect extent of fresh Ag nanoparticles is decreased. So it is easy to understand that Raman intensity is close to the maximum as the laser irradiation time is prolonged to 50 s. In a word, the defect extent and the proportion of fresh Ag could be directly responsible for the evolution of Raman signals. Combined with the analysis for laser-driven evolution, a visual and concise schematic illustration was shown in Fig. 5 to illustrate the process of in situ obtaining SERS signals.

3.4. Evaluation for the strategy

Not only can the strategy of laser-driven obtaining of fresh Ag be used to detect on-line 4-Mpy molecules, but also applied to detect PATP molecules (see Supporting Fig. S3). As shown in Fig. S3, the SERS signals of PATP display a similar evolution with that of 4-Mpy. Besides, the stability of cubic AgCl nanoparticles is also crucial for their application in SERS, which determines whether AgCl can serve as precursors of SERS substrates or not for a long period. XRD results demonstrate that the cubic AgCl nanoparticles stored for 100 days in dark room still belong to a pure cubic phase [space group Fm-3 m] of AgCl (see Supporting Fig. S4), and no other phases were found. When the cubic AgCl nanoparticles stored for 100 days in dark room were chosen as precursors of SERS substrates, the enhancement trends and the position of vibration bands of 4-Mpy are highly similar with those Fig. 4 exhibits except that the overall intensity decreases (Fig. 6).

4. Conclusion

A facile strategy has been reported to obtain on-line fresh Ag as SERS active substrates by making AgCl nanoparticles exposed to the laser beam of Raman spectrometer [16,17]. The laser-driven evolution and possible formation mechanism of cubic AgCl nanoparticles to Ag/AgCl composites were amply investigated by TEM, EDS and HRTEM. It was found that the laser with high-energy intensity plays a vital role in the appearing of fresh Ag and the achievement of stable Ag/AgCl composites in a short time. This strategy of obtaining fresh Ag displays a prominent SERS sensitivity to probe molecules, such as 4-Mpy or PATP molecules. Raman measurements show that Raman intensity is close to a maximum when the laser irradiation time is prolonged to 50 s, which corresponds to the defect extent and the proportion of fresh Ag. This strategy applied to obtain on-line fresh Ag and detect organic molecules is simple, efficient and feasible.

Acknowledgments

This work was supported by the National Natural Science Foundation of China (No. 20873153), the National Basic Research Program of China (2011CB302103) and the State Key Laboratories of Transducer Technology for financial support (Skt0906).

Appendix A. Supplementary material

Supplementary data associated with this article can be found, in the online version, at doi:10.1016/j.jcis.2011.09.052.

References

- [1] M. Fleischmann, P.J. Hendra, A.J. McQuillan, *Phys. Chem. Lett.* 26 (1974) 163.
- [2] S.M. Nie, S.R. Emory, *Science* 275 (1997) 1102.
- [3] Z.Q. Tian, B. Ren, D.W. Wu, *J. Phys. Chem. B* 106 (2002) 9463.
- [4] S.J. Lee, A.R. Morrill, M. Moskovits, *J. Am. Chem. Soc.* 128 (2006) 2200.
- [5] J.X. Fang, Y. Yi, B.J. Ding, X.P. Song, *Appl. Phys. Lett.* 92 (2008) 131115.
- [6] X.F. Liu, C.H. Sun, P. Jiang, *J. Phys. Chem. C* 113 (2009) 14804.
- [7] H.Y. Liang, Z.P. Li, W.Z. Wang, Y.S. Xu, H.X. Xu, *Adv. Mater.* 21 (2009) 4614.
- [8] A. Campion, P. Kambhampati, *Chem. Soc. Rev.* 27 (1998) 241.
- [9] M. Moskovits, *Rev. Mod. Phys.* 57 (1985) 783.
- [10] Q. Zhang, W.Y. Li, L.P. Wen, J.Y. Chen, Y.N. Xia, *Chem. Eur. J.* 16 (2010) 10234.
- [11] J.D. Driskell, S. Shanmukh, Y.J. Liu, S.B. Chaney, X.J. Tang, Y.P. Zhao, R.A. Dluhy, *J. Phys. Chem. C* 112 (2008) 895.
- [12] R.M. Liu, M.Z. Si, Y.P. Kang, X.F. Zi, Z.Q. Liu, D.Q. Zhang, *J. Coll. Interf. Sci.* 343 (2010) 52.
- [13] B. Zhang, A.W. Zhao, D.P. Wang, H.Y. Guo, D. Li, M. Li, *Chem. J. Chin. Univ.* 31 (2010) 1491.
- [14] M.F. Zhang, A.W. Zhao, H.Y. Guo, D.P. Wang, Z.B. Gan, H.H. Sun, D. Li, M. Li, *CrstEngComm.* (2011), doi:10.1039/C1CE05105A.
- [15] J.L. Gong, J.H. Jiang, Y. Liang, G.L. Shen, R.Q. Yu, *J. Coll. Interf. Sci.* 298 (2006) 752.
- [16] H.G. Zhang, F.C. Liu, T.J. He, H.W. Xin, *Spectrochimica. Acta. Part A* 51 (1995) 1903.
- [17] M. Voikan, D.L. Stokes, T. Vo-Dinh, *Sens. Actuat. B* 106 (2005) 660.
- [18] C. Yang, Y.T. Xie, M.F. Yuen, X.M. Xiong, C.P. Wang, *Phys. Chem. Chem. Phys.* 12 (2010) 14459.
- [19] C.H. An, S. Peng, Y.G. Sun, *Adv. Mater.* 22 (2010) 2570.
- [20] H.X. Xu, E.J. Bjerneld, M. Käll, L. Börjesson, *Phys. Rev. Lett.* 83 (1999) 4357.
- [21] H.L. Hu, W. Song, W.D. Ruan, Y.F. Wang, X. Wang, W.Q. Xu, B. Zhao, *J. Coll. Interf. Sci.* 344 (2010) 251.
- [22] W. Song, Y.X. Wang, B. Zhao, *J. Phys. Chem. C* 111 (2007) 12786.